IET Circuits, Devices & Systems

Research Article

IET Journals
The Institution of Engineering and Technology

Indirect and adaptive test of analogue circuits based on preselected steady-state response measures

ISSN 1751-858X
Received on 6th May 2019
Revised 12th January 2020
Accepted on 20th February 2020
E-First on 1st June 2020
doi: 10.1049/iet-cds.2019.0191
www.ietdl.org

Álvaro Gómez-Pau[1] ✉, Emili Lupon[1], Luz Balado[1], Joan Figueras[1]

[1]*Department of Electronics Engineering, Universitat Politècnica de Catalunya (UPC), Av. Diagonal, 647, 9th floor, 08028 Barcelona, Spain*
✉ *E-mail: alvaro.gomez-pau@upc.edu*

Abstract: Alternate testing techniques have been progressively adopted as a promising solution due to their effectiveness against classical specification-based test methods. This work presents a built-in test system, which adaptively generates an indirect digital signature characterising the circuit under test, which is later used to diagnose the actual performances relying on a statistical dictionary-based diagnosis method. The system is composed of an integrated digital signature generator and a digital control and acquisition subsystem. The signature generator is based on a converter architecture, in which the analogue range can be adapted to the magnitude of the indirect measure using the well known information of the fault-free circuit. The digital subsystem controls the proposed architecture and stores the digital codes sent by the integrated digital signature generator. The digital signature generator has been designed and fabricated in an industrial 65 nm complementary metal–oxide–semiconductor technology from STMicroelectronics, whereas the digital control and acquisition subsystem have been prototyped in a field-programmable gate array. The fabricated system has been used to test a biquad filter affected by parametric variations. Successful experimental results are reported showing the capabilities of the proposed adaptive test system to diagnose circuit performances with discrepancies as low as 1% of the actual real value.

1 Introduction

Testing analogue and mixed-signal circuits is a challenging task due to the limitations of current analogue automatic test equipment (ATE) and the partial availability of systematic procedures. These facts cause a significant increase of the incurred test costs, which are reflected in the final product [1, 2]. To partially overcome these drawbacks, indirect testing techniques have been widely used in contrast to the classic specification-based test approaches [3–5]. Indirect testing strategies solely rely on easy to measure parameters to perform the test. The set of indirect measurements used to perform the test usually has a certain correlation with the circuit performances to be validated. Basically, two different approaches can be found in the literature. One possibility is to map each of the easy to measure parameters to each of the performances. This is usually achieved by using regression techniques, such as multivariate linear regressions or even using a more advanced approach via the well known multi-adaptive regression splines models [3, 6]. Another possibility is to identify the non-linear test decision boundary in the indirect measurement space. To that purpose, among other existing methods, octrees have been lately proposed to digitally encode the indirect measurements space and evaluate a candidate circuit with low-test application times as well as low-memory overhead [7]. Machine-learning strategies are, in general, a well-suited approach with promising results in the field [8–10].

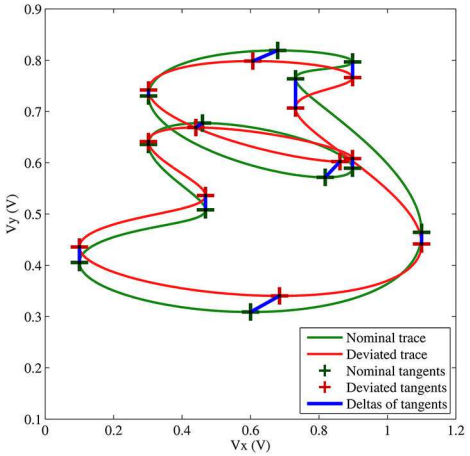

Fig. 1 *Nominal and deviated analogue signatures resulting from an XY signal composition. The extreme points of the traces contain the signal information, which serves for test/diagnosis purposes in this work [7, 11, 12]*

The use of analogue signal composition was proposed in the past as a successful indirect testing strategy [11]. As an example, consider the *XY* composition shown in Fig. 1. The green trace corresponds to the nominal signature generated when a linear time invariant filter is excited with a multitone signal. The red trace corresponds to the same composition but with the circuit under test (CUT) being affected by a parametric deviation, usually due to fabrication process variations. As can be observed, both signatures clearly differ from each other; therefore, allowing to identify component deviations or functional misbehaviour using such compositions together with an appropriate method to quantify the deviation level. A methodology for compacting the analogue signature provided by the *XY* composition has been proposed in [12]. It relies on the displacement of the tangency points of the trace to horizontal and vertical tangent lines, as depicted in Fig. 1. Using the Lissajous trace tangency points allows the extraction of sufficient CUT information to perform the test, yet keeping the shape of the *XY* composition for further exploration.

This work is based on the previous idea but extending the concept of arbitrary signal monitoring to a built-in proposal. The proposed architecture conforms the so-called adaptive signature generator system, which monitors analogue signals and generates a digital signature containing the necessary information to diagnose the defect level and/or pass/fail status of the CUT. The proposed monitor relies on an adaptive observation window for each of the alternate measurements, which can be adjusted depending on the expected variability and the desired acquisition resolution when generating the digital trace information. The feasibility of the adaptive monitoring system has been experimentally assessed by using a biquad filter affected by parametric defects. This work only focuses on parametric defects (process, voltage, temperature or

```
1: function SELECTMEASUREMENTS(M, n, k)
2:     Precond: M is a candidate set of n measurements
3:     Precond: k is the number of measurements to choose
4:     for μ ← AllCombinations(n, 2) do
5:         T_μ ← KendallTau(M_μ)
6:     end for
7:     ᾱ ← ∞
8:     for ν ← AllCombinations(n, k) do
9:         Γ ← ∅
10:        for μ ← AllCombinations(ν, 2) do
11:            push(Γ, T_μ)
12:        end for
13:        α ← Mean(Γ) + Stdev(Γ)
14:        if α < ᾱ then
15:            ᾱ ← α
16:            ν̄ ← ν
17:        end if
18:    end for
19:    return ν̄
20:    Postcond: ν̄ contains the indexes of the selected k
21:              indirect measurements
22: end function
```

Fig. 2 *Algorithm to select a subset of indirect measurements for mixed-signal testing. The measurements within the resulting subset minimise the average value and spread of their pairwise Kendall's Tau statistic*

ageing) and assumes catastrophic faults have been detected in a previous test tier.

The work is organised as follows. Section 2 focuses on two important considerations when using any alternate testing methodology, namely the selection of the alternate set of indirect or alternate measurements and how the information provided extracted from these measurements is processed in order to derive a reliable test decision. The selection of measurements is carried out via an algorithm having the goals of minimising the redundancy between alternate measurements. The diagnosis procedure is based on a sparse dictionary technique allowing a robust and efficient diagnosis of the sought-for circuit performances. Section 3 presents the adaptive signature generator system based on signal monitoring. The proposed architecture can monitor signals within the so-called observation windows and generate indirect digital signatures to be used for test or diagnosis purposes. The proposed architecture can be easily generalised to *n*-dimensions despite here, and for the sake of simplicity, only two dimensions will be considered. The presented adaptive signature generator system is composed of two subsystems: the integrated digital signature generator subsystem and the digital control and acquisition subsystem, which are also explained in detail. Section 4 is devoted to show the viability of the proposed and fabricated signature generator when it is experimentally applied to diagnose and test a low-pass biquad filter affected by parametric deviations. Finally, Section 5 summarises the results and concludes this paper.

2 Selection of steady-state measures and the diagnosis procedure

As mentioned before, when it comes to the implementation of a new alternate testing methodology, one of the key aspects, amongst others, is to perform an adequate selection of alternate measurements. The selection of these measurements is of vital importance since it will determine the effectiveness of the testing methodology both in terms of accuracy as well as test application time, which directly impacts the cost of the mixed-signal test. Equally important is the way the information provided by the selected alternate measurements is processed in order to derive a reliable and trustworthy test decision. In this work, a sparse dictionary technique is used. Such an approach allows the reduction of dictionary memory requirements, whereas achieving an adequate accuracy since the diagnosed performance results from the solution of an overdetermined system of equations using least squares via the Moore–Penrose pseudoinverse. Further explanations of these two key aspects of alternate test are found throughout the rest of this section.

2.1 Indirect measurements selection criterion

This section introduces the used statistic to efficiently perform the selection of a subset of indirect measurements [13]. From now on, it will be referred to as the *selection statistic* or the *α-statistic*. Alternate testing strategies require the selection of a set of easy to measure parameters to be used as indirect measurements. To that purpose, many options exist, some of them entirely relying on the designer's expertise and experience. Some authors have proposed the use of the sensitivity matrix between the circuit's functional specifications and indirect measurements to maximise its rank [14, 15]. Statistical methods have also been proposed; most of them relying on correlations and regressions techniques between the set of functional specifications and the set of indirect measurements. For instance, in [16, 17], Barragan, Leger and Leger, Barragan used the Brownian distance correlation together with a greedy algorithm in order to select a meaningful subset of measurements adequate for analogue/radio-frequency circuits testing.

The selection of indirect measurements is a challenging issue since the relationship of the information provided by the indirect measurements to the actual functional performances to validate is not straightforward. The key idea is to perform the selection, trying to avoid or reduce redundancy between the measurements. This fact implies the achievement of a balance between the amount of relevant circuit information available at the testing time and the incurred tests costs tied to redundant measurements. According to this reasoning, a subset of indirect measurements for analogue and mixed-signal testing should accomplish the following two properties. The measurements need to reflect the circuit's functional specifications variability in order to allow the test to be performed efficiently and should not be redundant to avoid incurring in extra tests costs yet providing the crucial information.

This section extends the previous concepts to the scenario, in which more than two indirect measurements are required to perform the test. The algorithm listed in Fig. 2 describes the required steps to select an adequate subset of k indirect measurements out of a candidate set of n measurements according to the criteria discussed above. To achieve this goal, the method relies on a pairwise correlation statistic (Kendall's Tau coefficient in this case [7, 18]). These pairwise correlations are computed and stored in matrix $\boldsymbol{T}_{\mu}$, being μ a set of the two indexes of measurements involved in the correlation computation. Then, all the possible combinations of k indirect measurements are explored, and for every subset the selection statistic or α-statistic is computed. Each of the subsets is formed by the k indexes within the ν set. As introduced before, the α-statistic is computed by adding the expectancy and standard deviation of all the pairwise correlations within the current subset of indirect measurements. Finally, the subset of indexes $\bar{\nu}$ presenting the minimum α-statistic is returned. To select the minimum α-statistic, $\bar{\alpha}$ is initialised to a large value at the very beginning of the algorithm.

Note that the computational complexity of the algorithm reduces, in practice, to the computation of the pairwise correlation matrix (line 5 in the algorithm listed in Fig. 2) since it is of order $\mathcal{O}(n^2)$. All the remaining steps present no computational effort since they are just memory access to the previously computed $\boldsymbol{T}_{\mu}$ matrix. This work uses this selection algorithm in order to choose a subset of indirect measurements among a large candidate set of alternate measurements. In this work, the candidate set of indirect measurements correspond to the horizontal and vertical tangency points of the input/output Lissajous trace when the CUT is excited with a multitone signal as Fig. 1 illustrates. The selection of such points allows keeping track of the shape of the analogue signature when it is affected by parametric variations as well as providing information on the defect level [11, 12]. This approach is similar to the way handwritten signatures or fingerprints are systematically characterised by their minutiae patterns (i.e. feature points). The presented α-statistic is used to select a small subset of alternate measurements amongst all the horizontal/vertical Lissajous tangency points. The voltage measurements are taken when the

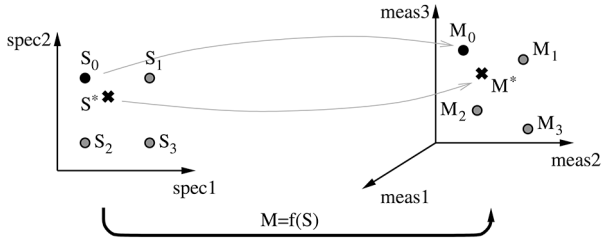

Fig. 3 *Sketch of the specifications and alternate measurements spaces, in which the diagnosis procedure is carried out via a sparse dictionary. The target specification $\boldsymbol{S}^\star$ is diagnosed using its corresponding $\boldsymbol{M}^\star$ alternate measurement as well as information of the surrounding dictionary points*

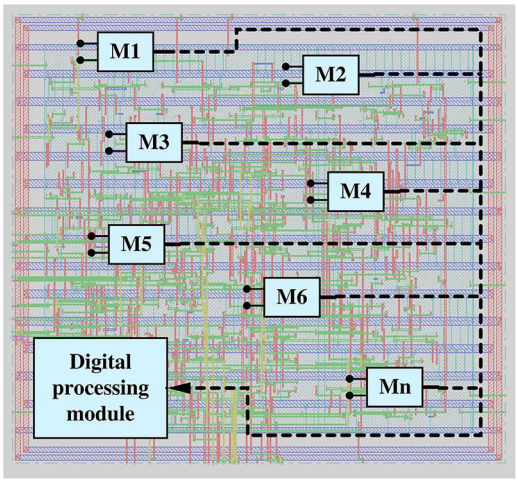

Fig. 4 *Integrated analogue signal monitoring and digital signature generation. The digital processing module facilitates the test/diagnosis decision based on the digital information provided by the monitors*

response of the CUT has achieved an oscillatory steady-state regime as will be further explained in Section 4.

2.2 Sparse dictionary-based diagnosis procedure

The diagnosis procedure is based on a sparse dictionary of precomputed performances–measurements pairs. The dictionary may be created relying on experimental measurements or Monte Carlo simulations. In this paper, the approach is to characterise the mapping between the alternate measurements space and the performances (i.e. specifications) in a sparse and uniform grid and use this information in order to infer the actual functional specifications given an alternate measurement. The sketch shown in Fig. 3 shows an example of these spaces as well as the sparse grid points (circles) contained within the dictionary together with a case example of inferred performances (crosses).

The way of dealing with the information contained within the dictionary is formalised as follows. Let us assume first there exist a, usually highly non-linear but continuous, function $\boldsymbol{M} = f(\boldsymbol{S})$, which maps these two spaces. From now on, n_s will note the dimensions of the specifications space and n_m will note the dimensions of the alternate measurements space $n_\mathrm{m} \geq n_\mathrm{s}$. Let us also assume the sparse dictionary is at our disposal containing information of performances and alternate measurements pairs; similarly, the data $(\boldsymbol{S}_0, \boldsymbol{M}_0)$, $(\boldsymbol{S}_1, \boldsymbol{M}_1)$, $(\boldsymbol{S}_2, \boldsymbol{M}_2)$, $(\boldsymbol{S}_3, \boldsymbol{M}_3)$ illustrated in Fig. 3. The generated dictionary should also contain information on the local slope at every specification point of the dictionary grid, that is, the Jacobian matrix of dimension $n_\mathrm{m} \times n_\mathrm{s}$; henceforth, noted as $\boldsymbol{J}$. Note that such a dictionary might be sparse and needs to be generated just once.

Given a vector of indirect measurements $\boldsymbol{M}^\star$, of dimension n_m, the goal is to determine its corresponding specifications vector $\boldsymbol{S}^\star$ of dimension n_s. Let us consider the closest point within the dictionary, the pair $(\boldsymbol{S}_0, \boldsymbol{M}_0)$ in the sketch of Fig. 3, so one may write the first-order Taylor series approximation particularised at $(\boldsymbol{S}_0, \boldsymbol{M}_0)$ and relating $(\boldsymbol{S}^\star, \boldsymbol{M}^\star)$

$$\boldsymbol{M}^\star = \underbrace{f(\boldsymbol{S}_0)}_{\boldsymbol{M}_0} + \boldsymbol{J}_0 \cdot (\boldsymbol{S}^\star - \boldsymbol{S}_0) \tag{1}$$

Note that the only unknown in (1) is $\boldsymbol{S}^\star$, and could be solved using generalised least squares via the so-called Moore–Penrose pseudoinverse of the Jacobian matrix, which is a non-square matrix, in general, like so

$$\boldsymbol{S}^\star = S_0 + (J_0^\mathrm{T} J_0)^{-1} J_0^\mathrm{T} \cdot (\boldsymbol{M}^\star - M_0) \tag{2}$$

It turns out that (2) should be the solution if the dictionary consisted of a single data point but there are many more available and close enough to the vector of alternate measurements $\boldsymbol{M}^\star$, which can actually improve the diagnosed performances. Let us assume that, instead of a single point, we consider the q closest dictionary points to $\boldsymbol{M}^\star$, so (1) should be expanded to a system of equations

$$\left.\begin{aligned} \boldsymbol{M}^\star &= \boldsymbol{M}_0 + \boldsymbol{J}_0 \cdot (\boldsymbol{S}^\star - \boldsymbol{S}_0) \\ \boldsymbol{M}^\star &= \boldsymbol{M}_1 + \boldsymbol{J}_1 \cdot (\boldsymbol{S}^\star - \boldsymbol{S}_1) \\ &\vdots \\ \boldsymbol{M}^\star &= \boldsymbol{M}_{q-1} + \boldsymbol{J}_{q-1} \cdot (\boldsymbol{S}^\star - \boldsymbol{S}_{q-1}) \end{aligned}\right\} \tag{3}$$

where, again, the only unknown is $\boldsymbol{S}^\star$ but in this case the diagnosis procedure is endowed with much more information than when just considering a single dictionary entry. The system of (3) can be rewritten in a more convenient way, becomes

$$\left.\begin{aligned} \boldsymbol{M}^\star - \boldsymbol{M}_0 + \boldsymbol{J}_0 \boldsymbol{S}_0 &= \boldsymbol{J}_0 \boldsymbol{S}^\star \\ \boldsymbol{M}^\star - \boldsymbol{M}_1 + \boldsymbol{J}_1 \boldsymbol{S}_1 &= \boldsymbol{J}_1 \boldsymbol{S}^\star \\ &\vdots \\ \boldsymbol{M}^\star - \boldsymbol{M}_{q-1} + \boldsymbol{J}_{q-1} \boldsymbol{S}_{q-1} &= \boldsymbol{J}_{q-1} \boldsymbol{S}^\star \end{aligned}\right\} \tag{4}$$

Let us rename the left-hand sides of these equations by a single vector $\widetilde{\boldsymbol{M}}$ of dimension $n_\mathrm{m} \cdot q$ and the stack of Jacobians by $\widetilde{\boldsymbol{J}}$ which will have dimension $(n_\mathrm{m} \cdot q) \times n_\mathrm{s}$. According to these notations, the resulting diagnosed performances considering the q closest dictionary entries can be computed in a similar way derived in (2)

$$\boldsymbol{S}^\star = (\widetilde{\boldsymbol{J}}^\mathrm{T} \widetilde{\boldsymbol{J}})^{-1} \widetilde{\boldsymbol{J}}^\mathrm{T} \cdot \widetilde{\boldsymbol{M}} \tag{5}$$

The previous expression is used to perform the diagnosis procedure once the set of q nearest dictionary data points are identified. The combination of a sparse dictionary technique together with a mathematical refinement allows a fast, low-cost and effective approach to the diagnosis of analogue and mixed-signal circuits.

3 Adaptive signature generator system proposal and design

As mentioned in Section 1, testing analogue circuits in mixed-signal integrated circuits (ICs) is an arduous and costly task due to the demanding test time targets. Testing the analogue part of a circuit, which represents a small portion of the total silicon area, results in large test costs due to time consumption and non-standardised test techniques. One possibility to cope with these problems is to use indirect testing strategies together with analogue signal monitoring [11]. This allows the generation of a set of digital signals characterising the CUT, which are delivered to the digital ATE. The digital output can be a pass/fail signal or a more complex digitally encoded analogue measurement. Fig. 4 shows a complex mixed-signal IC structure including some of such monitors capable of generating signatures of the analogue circuitry. A digital

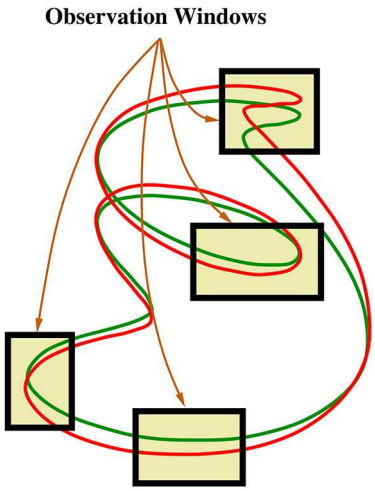

Fig. 5 *Composition of two analogue signals and four possible observation windows. Each observation window focuses on a certain area of interest, based on a previous sensitivity/correlation analysis [13]*

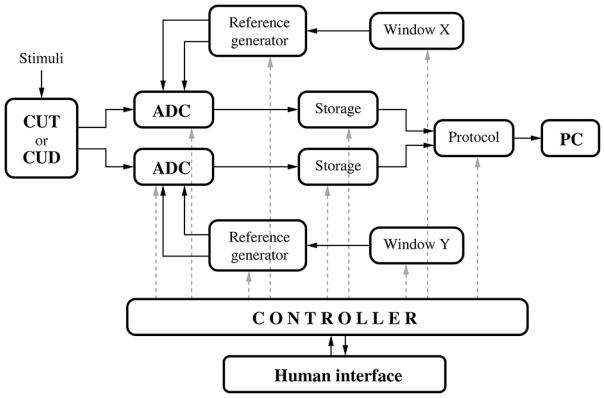

Fig. 6 *Basic architecture of the signature generator system. CUT/CUD analogue signals are monitored and digitised within the observation window limits established by the controller. In this work, the data are stored and transferred to a PC for further processing*

processing module is in charge of combining and generating the required information for testing the analogue circuitry.

The new approach presented in this work is based on an adaptive monitor, intended for testing and diagnosis purposes. The presented monitor samples two analogue signals within an *acceptance/observation window* and delivers a digital signature of these signals in two different ways. First, it acts as an indicator stating whether the signal is inside or outside the acceptance window. Second, when the signal is inside the acceptance window, the monitor delivers an *n*-bit resolution digital measurement of the analogue signals being monitored. This idea comes from the fact that, in a parametric testing scenario, the values to be measured are known to be close to the values measured in the golden or defect-free circuit. Since the accepted tolerances due to parametric deviation are also known, it is possible to design, as part of the testing system, a specific converter that can be adapted to these previously known ranges.

For the particular case of *XY* testing, the resulting composition becomes the analogue signature of the CUT/circuit under diagnosis (CUD). Variations in circuit parameters will shift and twist the curve resulting, for instance, in the red trace shown in Fig. 1, as opposed to the nominal green trace. The location of the observation windows are determined by the selection of the more sensitive tracepoints and/or the ones with higher correlation with specifications. Fig. 5 represents four of such windows. To implement the proposed signature generator, two adaptive analogue-to-digital converters (ADCs) are needed. These converters digitise the signals with *n*-bit resolution within the range of the established observation windows, which may be different for each of the axis. Outside the observation window, the converter is out of scale and yields all zeroes or all ones depending whether the value is below or above the observation window. Within the window range, the converter delivers the digitised values of the analogue signals being monitored. It can be easily understood as a zoom of the signal within the acceptance window. Therefore, a converter with less resolution and with less complexity and size can be used for this purpose since the actual resolution is increased as the window range is shrunk.

The observation windows are configured by setting the reference voltages to adequate values according to the alternate information to measure. The analogue range established by these references becomes the rail-to-rail input range to the analogue comparators in order to take full advantage of the available resolution of the converter. The system acts like a zoom-in within the measure of interest, which allows obtaining good resolutions with a relatively low number of bits. The system may also be used with diagnosis purposes within the observation window ranges as well as with testing purposes if the trace does not enter within the observation windows. This reduction of complexity allows more traces to be monitored in order to guarantee the test and/or diagnosis results with the same overhead.

The complete architecture of the proposed signature generator is shown in Fig. 6. Besides the two adaptive flash converters composing the integrated signature subsystem, a digital control subsystem is also needed to manage the converters, establish the adaptive observation windows references and process the generated digital signatures. The interface between the digital and analogue parts is a single bit serial transmission carrying the digitised values of the two analogue signals being monitored. This information is decoded and stored or transferred for internal digital post-processing or delivered to external ATE resources. Next sections describe both the integrated and the digital signature generator subsystems.

3.1 Integrated signature generator subsystem

The integrated digital signature generator subsystem is in charge of providing the digitised information of the analogue traces being monitored within the observation windows.

Fig. 7 shows the architecture of one of the channels conforming the integrated signature generator proposed in this work. It is composed of a flash ADC structure with serial output capabilities. The flash ADC references are generated by an active voltage divider constructed using isolated *n*-well P-channel metal–oxide–semiconductor (PMOS) transistors, what yields to a low-power structure as well as a compact design, as opposed to the classical polysilicon resistor ladder. In addition, taking advantage of the metal-insulator-metal (MiM) capacitor capabilities provided by the technology, stabilisation capacitors have been included in the design to reduce voltage variations in reference nodes.

The integrated signature generator subsystem functions as follows. Each of the comparators compares the analogue input signal with respect to the voltage references generated by the established observation window limits and the active voltage divider. Every time shift registers parallel load signal (active low), negated of load signal (NLD) is activated at a rising clock edge, the digital thermometric code is stored in the flip-flops and the first least significant bit (LSB) bit is flushed to the output. Ever since every rising edge clock pulse makes the shift register continue flushing its contents until all the thermometric information is sent to the digital control and acquisition subsystem. Then, the cycle starts over again with the next sample.

The integrated digital signature generator subsystem has been designed and fabricated in an industrial 65 nm complementary MOS (CMOS) technology from STMicroelectronics using Cadence custom IC design tools. Fig. 8 shows the layout of the two-channel signature generator, which is 170 μm wide and 62 μm high, resulting in a total silicon area of 10,540 μm^2. As pointed earlier, both channels are composed of an array of comparators capable of providing the thermometric code of the sampled signal. Fig. 9 shows the detailed layout of one of these comparators. The comparators have been designed with rail-to-rail input and output as well as using common centroid design techniques [19] in order

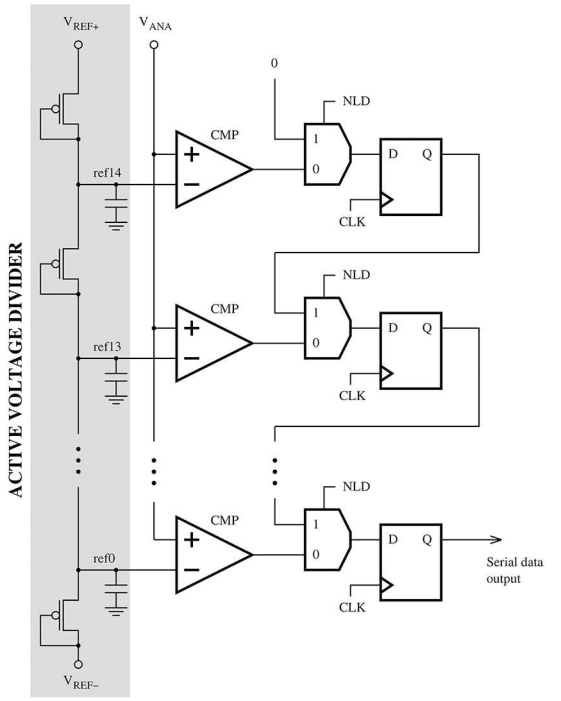

Fig. 7 *Schematic representation of the integrated signature generator subsystem. Internal ADC references are generated using a diode-connected, isolated n-well, PMOS transistor ladder. Comparator outputs are serially transmitted to the FPGA-based digital control and acquisition subsystem*

Fig. 8 *Layout of the integrated signature generator subsystem (both channels), where the array of comparators can be appreciated as well the active voltage divider and the shift register structure. The integrated signature generator subsystem is 170 µm wide and 62 µm high (10,540 µm^2) and has been designed and fabricated in an industrial 65 nm STMicroelectronics bulk CMOS technology*

to reduce transistor mismatch, especially in those requiring a perfect match such as the input differential pair or current mirror sources. The dimensions of the comparator are 9.6 µm wide and 8.7 µm high, yielding a total comparator area of about 83.5 µm^2. Fig. 10 shows a photograph of the fabricated multi-project bare die, in which the integrated digital signature generator subsystem can be identified (the two golden rows in the upper-left corner of the die). Fig. 11 shows the encapsulated die mounted in the printed circuit board.

3.2 Digital control and acquisition subsystem

The digital control and acquisition subsystem aims to serve as a suitable interface between the integrated signature generator digitising the *XY* pairs and the digital ATE equipment. In this work, a computer will play the role of the ATE equipment by processing the signatures and taking the test decision based on the sparse dictionary technique presented earlier. To this purpose, the digital control and acquisition subsystem is in charge to perform the following tasks:

- Establish the observation window.
- Control the digital signature generator serial transmission of the digitised *XY* pairs. Each pair consists of 30 bits of data (i.e. two 15 bit thermometric codes).
- Receive the *XY* pairs and compact them to binary code.
- Store the consecutive *XY* pairs related to the observation window.
- Send the stored *XY* pairs to the computer for further analysis and inferring the circuit performances.

As a fast prototype, all the logic required to perform these tasks has been described in very high speed integrated circuit hardware description language and implemented in an field-programmable gate array (FPGA) from Intel (formerly Altera). A Terasic DE0 development board including a Cyclone III EP3C16F484C6 device has been used. The use of this board has additional advantages since it already includes a 50 MHz oscillator generating the clock signal driving the FPGA, a universal serial bus (USB) connection which has been used to interface with the PC, and a user interface composed of switches, light-emitting diodes and seven-segments displays to which several functions have been assigned as will be described in the following paragraphs.

An observation window is defined by four voltage references, namely the top and bottom voltage references for the first channel and the top and bottom voltage references for the second channel. These voltage references must be delivered to the digital signature generator and can be obtained through appropriate digital-to-analogue converters (DACs) controlled by the digital control and acquisition subsystem. In this way, an observation window is defined by four digital values. Successive sets of these four values can be established on the fly through the above-mentioned user interface and stored within the RAM of the device or, alternatively, they can be established at compilation time and stored within the RAM of the device at a power-on time (the power-on initialised RAM operates as a ROM). The observation window resolution has been established to 1/64th of the total voltage range, so six bits are enough to set each of the aforementioned voltage references.

To minimise the cost of the DACs, each DAC has been implemented as inverted weight outputs inverted weight output counter (IWOC) digital pattern generator [20] followed by a first-order low-pass filter. The IWOC digital pattern generator has an architecture similar to a PWM generator based on an n-bit binary counter and an n-bit comparator but inverting the weights of the counter bits before the comparison (i.e. bits i and $n-1-i$ are swapped). Fig. 12 shows the architecture of such DAC structure for $n = 6$, allowing to define the voltage references for the observation window in steps of 18.75 mV. The frequency of the DAC clock is 50 MHz and the cut-off frequency of the low-pass filter is about 1.1 kHz, guaranteeing a ripple lower than 0.5 mV. Note that the n-bit counter can be shared by the four DACs (Fig. 13).

By means of a frequency divider, a 1 MHz clock is generated by the FPGA internal logic for controlling the digital signature generator serial transmission of the sampled *XY* pairs. A low-level pulse of the NLD signal is generated every 30 clock periods to allow loading the sampled *XY* pairs in the shift register for their serial transmission to the PC. As highlighted before, the *XY* pairs are received in thermometric code chunks of 15 bits and, on the fly, converted to a 4 bit natural binary code. To store the consecutive *XY* pairs related to the observation window and send them to the PC through an USB connection, the SignalTap II Logic Analyser tool available within the software has been used. This debugging tool allows to include in the FPGA a logic analyser that samples the desired signals, stores them within the RAM and sends them through an USB connection for further processing. Using this tool, it is just necessary to sample the 4 bit registers storing the sampled data every 30 clock periods once the observation window is reached.

4 Experimental results

To show the viability of the proposed adaptive test/diagnosis system, it has been applied to diagnose and test a low-pass biquad filter affected by parametric deviations. The filter has been tuned at $f_0 = 1$ kHz with unity DC gain and critical damping ratio. The applied stimulus is a multitone signal composed of filter's characteristic frequency plus two extra tones: one octave higher and one octave lower. Such rich selection of tones can excite the

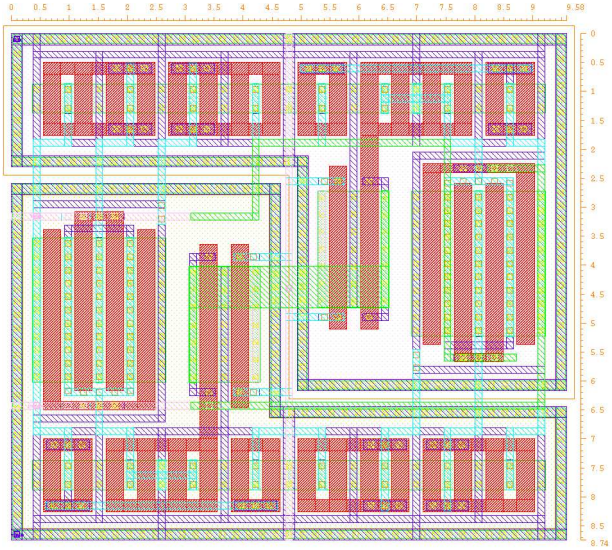

Fig. 9 *Detail of the designed analogue comparator included within the integrated signature generator subsystem. The design uses common centroid design methodologies in order to reduce transistor mismatch effects [19]. The comparator has both input and output rail-to-rail capabilities along the whole voltage operation range*

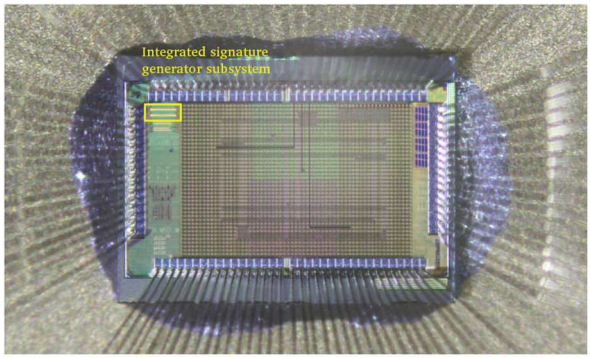

Fig. 10 *Photograph of the integrated signature generator subsystem fabricated in an industrial 65 nm CMOS technology. The integrated signature generator subsystem is 170 μm wide and 62 μm high (10,540 μm^2)*

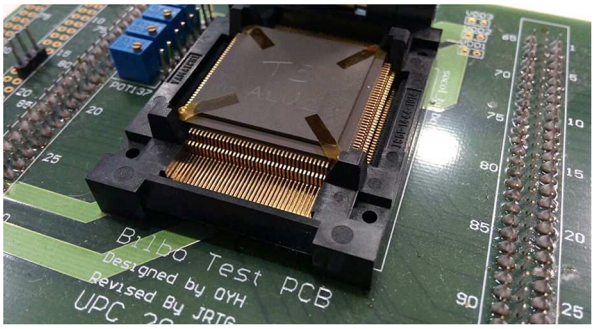

Fig. 11 *Detail of the 144 pads encapsulated version of the fabricated IC mounted on the socket and soldered to the test printed circuit board*

passband and the attenuation band of the filter; therefore, being able to manifest parametric deviations in circuit components.

As mentioned before, a previous study needs to be carried out in order to explore the *XY* composition. The resulting analogue signature information is compacted using its tangency points to horizontal and vertical lines, as depicted in Fig. 1 and exposed in Section 1. The displacements of these tangency points with respect to the nominal trace form the set of indirect testing measures. Among all the possible measures, two of them are selected using the criterion based on Kendall's Tau rank correlation coefficient [13] via the α-statistic, as explained in Section 2.

Once the indirect measures are selected, the observation windows ranges need to be established according to test specifications and the location of the nominal signature test points. The use of Monte Carlo simulations facilitates the appropriate selection of the acceptance/observation windows ranges according to the criteria exposed in Section 3. Fig. 14 shows the result of the conducted Monte Carlo simulations of the *XY* compositions together with the two selected tangency points determined by the α-statistic metric explained in Section 2. The tangency points of each Monte Carlo circuit are coloured in green for those accomplishing the specifications, whereas the ones violating them have been coloured in red. For the current case study, the selected observation window ranges are shown in Table 1, together with the digital code to be configured using the FPGA user interface.

The experimental setup is shown in Fig. 15. The integrated signature generator subcircuit is mounted on a board, which receives the *XY* analogue signals, the voltage references as well as the appropriate serial transmission control signals provided by the digital control and acquisition subsystem. The latter subsystem has been prototyped in a Terasic DE0 board and connected to a PC through an USB connection. The board between these two subsystems serves as a level conversion board as well as to physically support the first-order filters for the IWOC DACs.

The digital signature generator system functions as expected, as can be observed in the measured digital chronograms shown in Fig. 16. Once the NLD signal is activated (low) at a rising clock edge, comparator outputs in Fig. 7 are loaded into the shift register and the first LSB bit from channel *Y* is flushed to the output. Subsequent clock pulses continue flushing the digital data corresponding to channel *Y* and channel *X*, as shown in the chronograms of Fig. 16. Fig. 17 shows the measured Lissajous composition as seen on the oscilloscope before impedance matching. The experimental trace match the simulated trace shown in Fig. 1.

The digital data captured within the two observation windows used in this work are shown in Fig. 13. As expected, the experimental traces match the simulated *XY* composition within the ranges established by the observation windows. It can be appreciated the way the digital values saturate indicating the trace is outside the observation windows, yet providing the digital information within the acceptance window, as explained in Section 3.

To state the suitability of the developed adaptive signature generator system for test/diagnosis purposes, several amounts of deviations have been applied to filter's characteristic frequency ranging from 2.5 to 15%. For each of these deviated filters, *XY* composition data has been captured and processed. With the aim of denoising the data, several periods have been sampled and averaged (few milliseconds). Using a peak detection algorithm based on quadratic interpolation, the Δy displacements of the

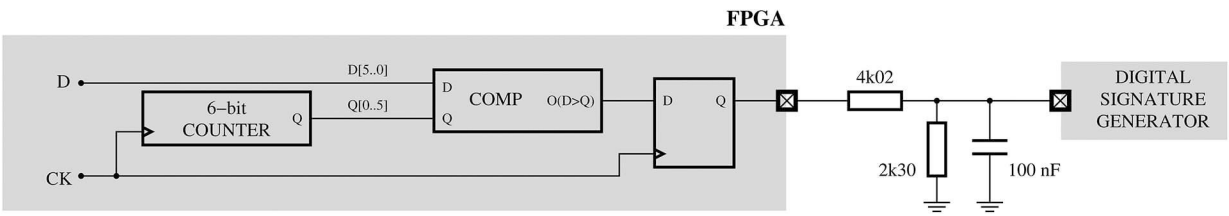

Fig. 12 *Architecture of the 6 bit DAC based on an IWOC digital pattern generator [20] as implemented in the digital control and acquisition subsystem. The use of four IWOC-based DACs allows the generation of the analogue limits for the observation windows as seen in Fig. 13*

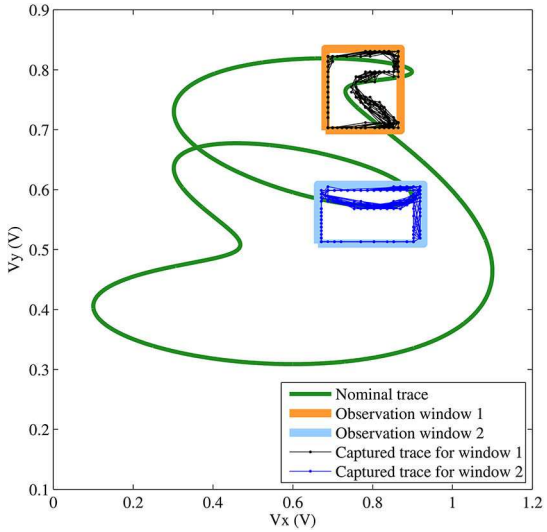

Fig. 13 *Simulated XY composition and the digitised experimental trace within the two observation windows considered in this work as defined in Table 1. As can be observed, the experimental traces match the simulated trace within both observation windows*

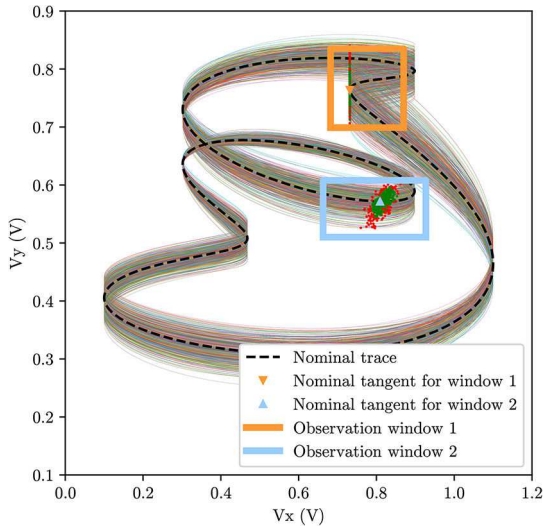

Fig. 14 *Monte Carlo simulations are showing the XY composition for the biquad filter used as a case study. The selected tangency points are also shown; the green ones correspond to circuits passing the specs, whereas the red ones correspond to circuits failing them*

Table 1 Established observation windows limits

	Window 1		Window 2	
Low	High	Low	High	
X range, mV	682 (0×24)	870 (0×2E)	663 (0×23)	927 (0×31)
Y range, mV	699 (0×25)	835 (0×2C)	510 (0×1B)	608 (0×20)

Lissajous traces have been measured within each of the observation windows. Table 2 shows these measurements and the inferred deviation level for each of the windows relying on the simulation data shown in Fig. 18. Finally, the diagnosed deviations for each observation window can be averaged to yield the diagnosed deviation level in filter's f_0 frequency. Table 2 also shows the relative error in diagnosing each of the applied deviation levels. As can be stated, all the reported errors (see Table 2) are in the order of 1%; therefore, validating the proposed adaptive test/diagnosis signature generator system. Of course, the diagnosed value can be used to test the CUT by simply comparing it against the test limit, which is, in this particular case study $\Delta f_{0\max} = 8\%$.

5 Conclusions

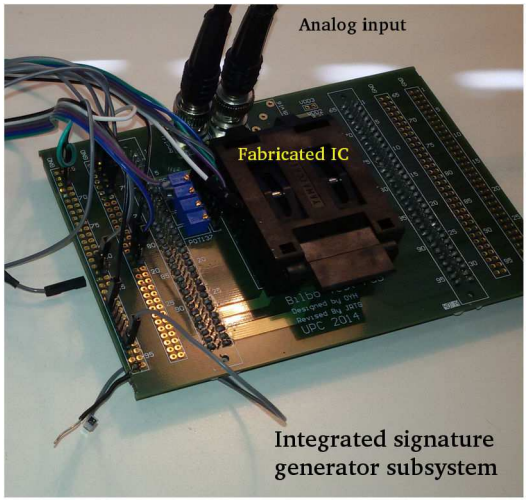

Fig. 15 *Photograph of the board containing the fabricated IC is implementing the integrated signature generator subsystem. Together with the digital control and acquisition subsystem implemented on an Intel Cyclone III FPGA board compose the proposed adaptive test system for analogue and mixed-signal circuits*

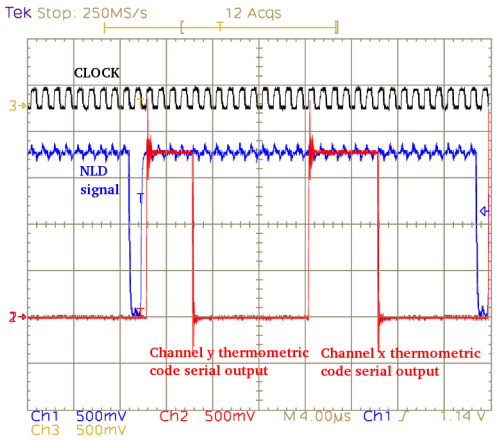

Fig. 16 *Oscilloscope chronograms of the signals involved in the serial transmission of the signature information. Once the load signal is activated, the shift register flushes the 15 bit thermometric code of both channels*

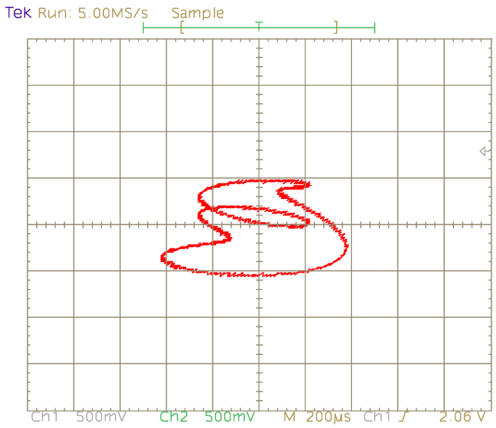

Fig. 17 *Measured Lissajous composition of the input/output signals when a multitone is applied to a low-pass biquad filter. As can be observed, the experimental Lissajous trace match the one shown in Fig. 1*

An adaptive signal monitoring system for mixed-signal test has been proposed. The key idea of the proposal is the monitorisation of the signal within predefined observation windows according to the expected location of the traces to observe, which has been previously selected using a correlation-based statistic. This allows the monitor to be adjusted to the signal limits, and therefore, to

Table 2 Diagnosis and test results

	Window 1		Window 2		Diagnosis/test results		
Δf_0, %	Δy_1, mV	Δf_{01}, %	Δy_2, mV	Δf_{02}, %	Δf_{0d}, %	Error, %	Test
2.50	6.97	2.34	−1.47	0.83	1.59	−0.89	pass
5.00	17.34	5.98	−8.70	4.95	5.47	0.44	pass
7.50	22.44	7.85	−13.84	7.93	7.89	0.36	pass
10.00	29.75	10.63	−17.15	9.87	10.25	0.23	fail
12.50	38.25	14.04	−19.48	11.25	12.65	0.13	fail
15.00	40.29	14.88	−20.52	11.88	13.38	−1.41	fail

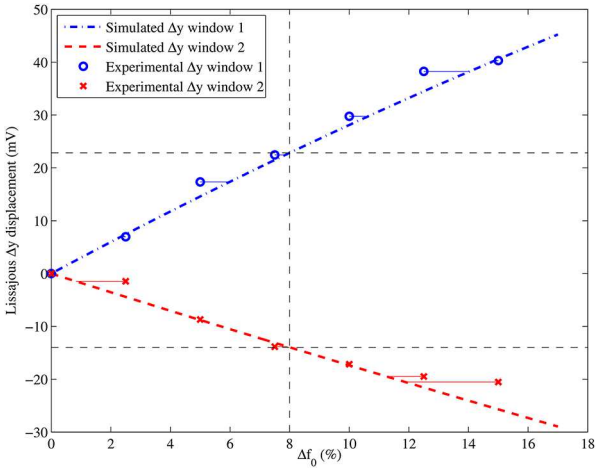

Fig. 18 *Simulated and experimental data of the* Δy *displacements of the two tangency points within each of the two observation windows considered in this work as the* f_0 *frequency of the filter varies from its nominal value*

increase the resolution with respect to a full range observation. The system is formed by an integrated signature generator subsystem and a digital control and acquisition subsystem. The former is composed of adaptive converters, which monitor the signal trace within the specified observation windows while the latter is in charge of establishing the observation windows limits and controlling the serial transmission of the acquired data, which is later further processed to take the test decision based on the diagnosed performances.

The integrated adaptive signature generator has been designed and fabricated in an industrial STMicroelectronics 65 nm CMOS technology, whereas the control and acquisition subsystem has been prototyped in an Intel Cyclone III FPGA. The system has been applied to diagnose and test a low-pass biquad filter affected by parametric deviations with the aid of a sparse dictionary-based diagnosis technique and statistical methods, which allow an effective selection of the indirect measurements to monitor and acquire. Successful experimental results have been reported showing a diagnosis discrepancy in the order of 1% when inferring the cutting frequency of the filter under test.

6 Acknowledgments

This work has been partially supported by the Spanish Ministry of Economics and Competitiveness, project reference TEC2013-41209-P and European Union FEDER funds.

7 References

[1] Milor, L.S.: 'A tutorial introduction to research on analog and mixed-signal circuit testing', *IEEE Trans. Circuits Syst. II, Analog Digit. Signal Process.*, 1998, **45**, (10), pp. 1389–1407

[2] Gil, V.G., Arteaga, A.J.G., Léger, G.: 'Assessing AMS-RF test quality by defect simulation', *IEEE Trans. Device Mater. Reliab.*, 2019, **19**, (1), pp. 55–63

[3] Variyam, P.N., Cherubal, S., Chatterjee, A.: 'Prediction of analog performance parameters using fast transient testing', *IEEE Trans. Comput.-Aided Des. Integr. Circuits Syst.*, 2002, **21**, (3), pp. 349–361

[4] Gielen, G.G.E., Rutenbar, R.A.: 'Computer-aided design of analog and mixed-signal integrated circuits', *Proc. IEEE*, 2000, **88**, (12), pp. 1825–1854

[5] Leger, G., Barragan, M.J.: 'Mixed-signal test automation: are we there yet?'. 2018 IEEE Int. Symp. Circuits and Systems (ISCAS), Florence, Italy, 2018, pp. 1–5

[6] Friedman, J.H.: 'Fast MARS'. Department of Statistics, Stanford University, 1993, 110

[7] Gómez-Pau, A., Balado, L., Figueras, J.: 'Efficient production binning using octree tessellation in the alternate measurements space', *IEEE Trans. Comput.-Aided Des. Integr. Circuits Syst.*, 2016, **35**, (8), pp. 1386–1395

[8] Stratigopoulos, H.G., Makris, Y.: 'Error moderation in low-cost machine-learning-based analog/RF testing', *IEEE Trans. Comput.-Aided Des. Integr. Circuits Syst.*, 2008, **27**, (2), pp. 339–351

[9] Barragan, M.J., Leger, G.: 'A procedure for alternate test feature design and selection', *IEEE Des. Test*, 2015, **32**, (1), pp. 18–25

[10] Barragan, M.J., Leger, G., Gines, A., *et al.*: 'On the limits of machine-learning-based test: a calibrated mixed-signal system case study'. Design, Automation Test in Europe Conf. Exhibition (DATE), Lausanne, Switzerland, 2017, pp. 79–84

[11] Balado, L., Lupon, E., Figueras, J., *et al.*: 'Verifying functional specifications by regression techniques on Lissajous test signatures', *IEEE Trans. Circuits Syst. I, Regul. Pap.*, 2009, **56**, (4), pp. 754–762

[12] Gómez-Pau, A., Balado, L., Figueras, J.: 'Diagnosis of parametric defects in dual-axis IC accelerometers', *Microsyst. Technol. J.*, 2015, **21**, (9), pp. 1855–1866

[13] Gómez-Pau, A., Balado, L., Figueras, J.: 'Criteria for selecting a subset of indirect measurements for analog testing'. Proc. Design of Circuits and Integrated Systems Conf. (DCIS), Granada, Spain, 2016

[14] Slamani, M., Kaminska, B.: 'Analog circuit fault diagnosis based on sensitivity computation and functional testing', *IEEE Des. Test Comput.*, 1992, **9**, (1), pp. 30–39

[15] Chatterjee, A., Cherubal, S.: 'Method for diagnosing process parameter variations from measurements in analog circuits'. US Patent App. 09/838, 404, 2002

[16] Barragan, M.J., Leger, G.: 'Efficient selection of signatures for analog/RF alternate test'. 2013 18th IEEE European Test Symp. (ETS), Avignon, France, 2013, pp. 1–6

[17] Leger, G., Barragan, M.J.: 'Brownian distance correlation-directed search: a fast feature selection technique for alternate test', *VLSI J. Integr.*, 2016, **55**, pp. 401–414

[18] Kendall, M.G.: 'A new measure of rank correlation', *Biometrika*, 1938, **30**, (1/2), pp. 81–93

[19] Long, D., Hong, X., Dong, S.: 'Optimal two-dimension common centroid layout generation for MOS transistors unit circuit'. IEEE Int. Symp. Circuits and Systems, 2005 ISCAS 2005, Kobe, Japan, 2005, vol. **3**, pp. 2999–3002

[20] Lupon, E., Balado, L.: 'Digital/analogue converter architectures for digital ASICs: a performance comparison'. Proc. Design of Circuits and Integrated Systems Conf. (DCIS), Barcelona, 1996